Activity Coefficients from Molecular Simulations using the OPAS Method

Maximilian Kohns,[1, a)] Martin Horsch,[1] and Hans Hasse[1]

University of Kaiserslautern, Laboratory of Engineering Thermodynamics, Erwin-Schrödinger Str. 44, D-67663 Kaiserslautern, Germany

A method for determining activity coefficients by molecular dynamics simulations is presented. It is an extension of the OPAS method (osmotic pressure for the activity of the solvent) developed in previous work for studying the solvent activity in electrolyte solutions. That method is extended here to study activities of all components in mixtures of molecular species. As an example, activity coefficients in liquid mixtures of water and methanol are calculated for 298.15 K and 323.15 K at 1 bar using molecular models from the literature. These dense and strongly interacting mixtures pose a significant challenge to existing methods for determining activity coefficients by molecular simulation. It is shown that the new method yields accurate results for the activity coefficients which are in agreement with results obtained with a thermodynamic integration technique. As the partial molar volumes are needed in the proposed method, the molar excess volume of the system water + methanol is also investigated.

[a)]Corresponding author; maximilian.kohns@mv.uni-kl.de; phone: +49-631 / 205-3216; fax: +49-631 / 205-3835.

I. INTRODUCTION

Chemical potentials or related properties like activities or activity coefficients are needed for the determination of phase equilibria, and therefore their computation is a commonly encountered task in molecular simulation studies. Most methods for determining the chemical potential in molecular simulations are based on particle insertion. Often, the test particle method of Widom[1] is used. However, in dense systems, that method tends to fail because of extremely high energies upon insertion of the 'ghost' particles. To overcome this difficulty, different elaborate sampling schemes have been suggested, e.g. the gradual insertion or thermodynamic integration techniques[2,3]. But still, for dense and strongly interacting systems, long simulations are usually required, and method-specific simulation parameters have to be determined by trial-and-error beforehand. Despite this, the methods may still turn out to be unfeasible.

In this work, a new approach for obtaining activity coefficients in the liquid phase in molecular dynamics simulations is presented. It builds on previous work of our group in which the OPAS method (osmotic pressure for the activity of the solvent)[4,5] was developed based on ideas described by Murad and co-workers[6–9]. In its previous version[4,5], the OPAS method was developed for determining the solvent activity in electrolyte solutions. In the present work, it is extended for determining activities of all species in mixtures of molecular species, similar to the approach of Crozier and Rowley[10]. To demonstrate the feasibility and accuracy of the new method, it is applied to determine activity coefficients in binary mixtures of water and methanol at 298.15 K and 323.15 K and 1 bar.

Binary mixtures of water and methanol have been the subject of many experimental and simulation studies. On the one hand, this is due to the importance of these substances

in many applications. On the other hand, as both water and methanol are strongly polar and hydrogen bonding, their mixture has often been used as a test case for thermodynamic models. The current version of the Dortmund Data Bank[11] lists more than 10,000 experimental data points for this system. Especially vapor-liquid equilibria and excess properties have been studied by many groups in a wide range of conditions. Mixtures of water and methanol have also been studied extensively using molecular simulation (e.g. in Refs. [10,12–41]). In most of these studies, the structure of the solution is investigated. Some publications also address hydrogen bonding statistics[12,13,18,28,29,38,41], excess properties[18–21,27,33,34,36,38–41] and transport properties[16,18,21,22,32,39,41]. In contrast, the number of molecular simulation studies of the vapor-liquid equilibrium or the related activity coefficients in the liquid phase is small[10,23,26,35], due to the fact that these properties are difficult to compute accurately in molecular simulations for dense liquid mixtures with strong interactions. Activity coefficients are derivatives of the free energy, so that they cannot be obtained by standard sampling and instead, special algorithms have to be designed for their calculation. As outlined above, most of the common algorithms to do so are based on particle insertions, which become very cumbersome for systems of strongly interacting particles.

In the present work, it is shown that the proposed extension of the OPAS method enables an accurate calculation of activity coefficients, even in challenging mixtures such as water + methanol. Since partial molar volumes are needed in the evaluation of the OPAS simulation results, the molar excess volume of the mixture is also investigated. To demonstrate the viability of the extended OPAS approach, we compare its results to results obtained with a thermodynamic integration technique.

The paper is structured as follows: In Section II, we briefly describe the employed molecular models. The rest of Section II is devoted to the derivation and presentation of the exten-

sion of the OPAS approach. This includes a procedure for obtaining partial molar volumes. In Section III, these volumetric properties are discussed first. Then, the OPAS simulation results are presented and compared to the results from thermodynamic integration, before we conclude in Section IV.

II. MOLECULAR MODELS AND SIMULATION METHODS

A. Molecular Models

In the present study, the TIP4P/2005 water model[42] and a methanol model from previous work of our group[43] are used. Both are known to give good predictions of pure component properties. Both models are rigid and non-polarizable and consist of Lennard-Jones (LJ) sites and partial charges. The potential is therefore

$$\begin{aligned} U &= U_{\mathrm{LJ}} + U_{\mathrm{CC}} \\ &= \sum_{i=1}^{N-1} \sum_{j=i+1}^{N} \left\{ \sum_{a=1}^{n_i^{\mathrm{LJ}}} \sum_{b=1}^{n_j^{\mathrm{LJ}}} 4\epsilon_{ijab} \left[\left(\frac{\sigma_{ijab}}{r_{ijab}} \right)^{12} - \left(\frac{\sigma_{ijab}}{r_{ijab}} \right)^{6} \right] + \sum_{c=1}^{n_i^e} \sum_{d=1}^{n_j^e} \frac{1}{4\pi\varepsilon_0} \frac{q_{ic} q_{jd}}{r_{ijcd}} \right\}. \end{aligned} \tag{1}$$

Here, a, b, c and d denote sites, i and j denote molecules, ε_0 is the vacuum permittivity, ϵ_{ijab} and σ_{ijab} are the Lennard-Jones energy and size parameters, r_{ijab} and r_{ijcd} are site-site distances, and q_{ic} and q_{jd} are the magnitudes of the partial charges.

To describe the interaction between unlike LJ sites, the Lorentz-Berthelot combining rules are used:

$$\sigma_{ijab} = \frac{\sigma_{iiaa} + \sigma_{jjbb}}{2}, \tag{2}$$

$$\epsilon_{ijab} = \sqrt{\epsilon_{iiaa} \epsilon_{jjbb}}. \tag{3}$$

B. Computation of Activity Coefficients with the OPAS Method

The OPAS method was developed in previous work with the aim of computing activities in electrolyte solutions. It is only introduced briefly here, for details, the reader is referred to our previous publications[4,5].

OPAS simulations are molecular dynamics simulations of the osmotic equilibrium between a pure component phase ($'$) and a mixture phase ($''$) which are in contact via a virtual semipermeable membrane. There is only one permeable component i. The membrane is realized in the simulation by applying an external force field on all molecules but those of component i to keep them inside the mixture phase ($''$), so that the phase ($'$) contains pure i. The osmotic pressure Π, which is the pressure difference between the two phases, is sampled as the membrane force per area.

In OPAS simulations, the temperature T and the pressure p' of the pure component phase are specified. The simulation results are the osmotic pressure Π and the composition of the mixture phase $\underline{x}$. The goal is the computation of the activity coefficient $\gamma_i(T, p', \underline{x})$ of the permeable component i at the specified temperature T and pressure p' as well as the composition of the mixture phase $\underline{x}$.

In the following, it is shown how $\gamma_i(T, p', \underline{x})$ is obtained. Normalizing the chemical potentials according to Raoult and rearranging the equilibrium condition for the osmotic equilibrium described above yields

$$\mu_i^{\text{pure}}(T, p'') - \mu_i^{\text{pure}}(T, p') = -RT \ln a_i(T, p'', \underline{x}). \tag{4}$$

Herein, μ_i and a_i are the chemical potential and activity of the permeable component i, and R is the universal gas constant. Combining Eq. (4) with

$$\mu_i(T, p', \underline{x}) = \mu_i^{\text{pure}}(T, p') + RT \ln a_i(T, p', \underline{x}) \tag{5}$$

$$\mu_i(T, p'', \underline{x}) = \mu_i^{\text{pure}}(T, p'') + RT \ln a_i(T, p'', \underline{x}) \tag{6}$$

yields

$$\mu_i(T, p'', \underline{x}) - \mu_i(T, p', \underline{x}) = -RT \ln a_i(T, p', \underline{x}). \tag{7}$$

Using $\Pi = p'' - p'$ this leads to

$$\int_{p'}^{p'+\Pi} v_i(T, p, \underline{x})\ dp = -RT \ln a_i(T, p', \underline{x}). \tag{8}$$

Splitting the activity a_i into the mole fraction x_i and the activity coefficient γ_i finally yields the desired relation

$$\ln \gamma_i(T, p', \underline{x}) = -\frac{1}{RT} \int_{p'}^{p'+\Pi} v_i(T, p, \underline{x})\ dp - \ln x_i. \tag{9}$$

In Eq. (9), T and p' are specified, and Π and x_i are OPAS simulation results. Additionally, the partial molar volume $v_i(T, p, \underline{x})$ is needed for the determination of the activity coefficient, and an integration over the pressure has to be carried out. In the present work, v_i was determined from the molar excess volume v^{E} as described in Section II C.

The relation between the activity and the osmotic pressure, cf. Eq. (9) has also been exploited in a recent paper by Smith et al.[44]. They, however, proceed in the opposite direction: A relation similar to Eq. (9) is employed to calculate the osmotic pressure in an electrolyte solution from knowledge of the solvent activity.

To obtain the N activity coefficients in a mixture of N components, N independent OPAS simulation runs have to be carried out. In each run, a different component i is treated as the permeable component, while all others cannot permeate the membrane. By the present method, the mixture phase composition $\underline{x}$ is not specified directly. Rather, the composition

is a simulation result. However, the initial conditions of the run can generally be chosen such that the final result for the composition is close to any desired value. The OPAS simulation runs are extremely simple, fast and robust compared to simulations employing particle insertion methods.

C. Computation of Molar Excess Volumes

The molar excess volume v^{E} of a mixture of N components is defined as:

$$v^{\mathrm{E}} = v - \sum_{i=1}^{N} x_i v_i^{\mathrm{pure}}, \tag{10}$$

where v is the molar volume of the mixture and v_i^{pure} are the pure component molar volumes. The molar excess volume is a function of temperature, pressure and composition: $v^{\mathrm{E}} = v^{\mathrm{E}}(T, p, \underline{x})$. In the present work, only binary mixtures of two components i and j are studied, so that Eq. (10) becomes

$$v^{\mathrm{E}} = v - x_i v_i^{\mathrm{pure}} - x_j v_j^{\mathrm{pure}}. \tag{11}$$

The molar excess volume is computed here by performing a series of simulations at different compositions in the NpT ensemble and applying Eq. (11). As the osmotic pressures obtained in OPAS simulations can reach very high values, cf. Section III B, such simulations are carried out at several isobars up to elevated pressures. For each isobar, the molar excess volumes can be correlated by a Redlich-Kister type expression:

$$v^{\mathrm{E}} = x_i x_j \left(A_0 + \sum_k A_k (x_i - x_j)^k \right), \; k = 1, 2, \ldots , \tag{12}$$

where A_0 and the A_k are fitting parameters. Adjusting Eq. (12) to the NpT simulation results is a standard polynomial regression. From that correlation, the partial molar volume v_i of component i can be obtained as

$$v_i = \left(\frac{\partial V}{\partial n_i}\right)_{T,p,n_{j\neq i}} = v_i^{\mathrm{pure}} + v^{\mathrm{E}} + x_j \left(\frac{\partial v^{\mathrm{E}}}{\partial x_i}\right)_{T,p,n_{j\neq i}} \tag{13}$$

where

$$\left(\frac{\partial v^{\mathrm{E}}}{\partial x_i}\right)_{T,p,n_{j\neq i}} = (x_j - x_i)\left(A_0 + \sum_k A_k (x_i - x_j)^k\right) + 2x_i x_j \left(\sum_k A_k k (x_i - x_j)^{(k-1)}\right),\ k = 1, 2, \ldots . \tag{14}$$

D. Details on the Simulations in the System Water + Methanol

In the present study, binary mixtures of water and methanol were considered. The aim was to determine activity coefficients at $p' = 1$ bar and either $T = 298.15$ K or $T = 323.15$ K over a wide concentration range. Details of the OPAS simulations and the standard NpT simulations for obtaining molar excess volumes are given in the Appendices A 1 and A 2, respectively. To validate the results for the activity coefficients determined with the OPAS method, they were also determined from independent simulations employing a thermodynamic integration technique[3,45]. Technical details of these simulations are given in Appendix A 3.

III. RESULTS AND DISCUSSION

Simulation results of the NpT simulations for obtaining the molar excess volumes are given in Table I, and the OPAS simulation results are given in Table II. Table III contains the results of the simulations using thermodynamic integration to validate our OPAS computations. In all tables, numbers in parentheses indicate the simulation uncertainties in the last given digit. The uncertainties for v^{E} were determined from error propagation of the simulation results for ρ via Eq. (11). The uncertainties in the evaluation of γ_i from the

OPAS results were then estimated by using the simulation results for v^{E} disturbed by their uncertainties in the correlation fitting, cf. Eq. (12), combined with error propagation of the uncertainty of Π. The uncertainties in the evaluation of γ_i from the simulations employing thermodynamic integration were estimated by error propagation of the simulation results for $\tilde{\mu}_i$, cf. Eq. (A2) in Appendix A 3.

Since the focus of the present work is to demonstrate the viability of the OPAS method, we discuss the comparison of the model predictions to experimental data only briefly.

A. Molar Excess Volumes and Partial Molar Volumes

First, the molar excess volumes of binary mixtures of water and methanol are discussed. The molecular simulation results are compared to correlations of experimental data for the two temperatures studied here in Fig. 1. The results of the predictive simulations with the Lorentz-Berthelot rules capture the trends of the experimental data reasonably. The location of the minimum in v^{E} at approximately equimolar composition is predicted correctly, however, its magnitude is underestimated by about 20%. The experimental data show that the difference between the two temperatures is almost negligible, and the molecular simulation results also capture this feature well. Quantitative agreement with the experimental data can probably be achieved by introducing an adjustable parameter in the mixing rules[20,27]. In the present work, however, our main concern is demonstrating the viability of the OPAS method for computing activity coefficients, and quantitative agreement with the experimental data is less important, so that we refrain from fitting binary interaction parameters.

Similar simulations were carried out at higher pressures. The simulation data were described by Redlich-Kister correlations, cf. Eq. (12). The results are shown in Fig. 2, the fit parameters are reported in Table I. Up to pressures of about $p = 10$ MPa, the pressure effect on

the partial molar volumes is small, but it becomes increasingly important at the elevated pressures. There, the partial molar volumes of both water and methanol exhibit a maximum. Comparing the two different temperatures, the curves are qualitatively similar. The main difference is a vertical shift of the curves resulting from the temperature dependence of the pure component molar volumes, which are in good agreement with the molar volumes computed from equations of state for both studied temperatures, cf. Fig. 2. A more detailed comparison of the partial molar volumes obtained from the simulations to experimental data is presented in the Supplementary Material.

B. Osmotic Pressures and Activity Coefficients

The osmotic pressures obtained by OPAS simulations at the two studied temperatures, using either water or methanol as the permeable component, are shown in Fig. 3. Simulations were carried out here for mole fractions above about 0.1 of the permeable component i in the mixture phase. At lower mole fractions of the permeable component, the statistics for the undisturbed mixture phase becomes poor for the present scenario. Fig. 3 shows that the osmotic pressure rises to very high values at low concentrations of the permeable component. Comparing the simulation results at the two temperatures shows that the temperature dependence of the osmotic pressures is very small. When evaluating activity coefficients from the OPAS simulations, the osmotic pressures are the upper bounds for the integration over the pressure in Eq. (9).

In order to evaluate the OPAS simulations to get activity coefficients, the partial molar volume of the respective permeable component was evaluated analytically at the composition of interest from the Redlich-Kister type correlations presented in Fig. 2. The resulting series of values at different pressures $v_i(p)$ was then fit to a polynomial of second degree.

This polynomial was integrated over the pressure in order to obtain the activity coefficients according to Eq. (9). The results are shown in Fig. 4 for both studied temperatures. The error bars for the activity coefficient obtained with the OPAS method are within symbol size. The OPAS data are smooth for both temperatures, and in the Supplementary Material, it is shown that the numbers for γ_{W} and γ_{MeOH} obtained from independent OPAS simulations are thermodynamically consistent. For $T = 323.15$ K, activity coefficients were also determined from sampling the chemical potential by thermodynamic integration in NpT simulations. The results are presented in Fig. 4, right panel, and in Table III. The data obtained by thermodynamic integration scatter much more strongly than those from the OPAS method, even though very long simulations were carried out, cf. Appendix A 3. At $T = 298.15$ K, thermodynamic integration breaks down due to the increased density. In contrast, the increased density at low temperatures has no effect on the performance of the OPAS method. Taking into account the uncertainties in the results obtained from thermodynamic integration, both simulation techniques agree well.

The data obtained from the investigated models qualitatively agree with the experimental results. However, together with the original Lorentz-Berthelot rules these models are not able to predict the activity coefficients quantitatively. Improvements could be achieved by parameter fitting, which is beyond the scope of the present work.

IV. CONCLUSIONS

An extension of the OPAS method is presented. It is based on the simulation of an osmotic equilibrium and enables accurate calculations of activity coefficients even in dense, strongly interacting mixtures. For every component i in the mixture, a set of OPAS simulations has to be carried out treating that component i as the permeable one. In the simulations,

the temperature T and the pressure p' in the pure component phase are specified and the activity coefficient γ_i at the composition of the mixture phase and at T and p' is determined. As high osmotic pressures are obtained, especially in simulations at high dilution of the respective permeable component, the pressure dependence of the activity coefficients has to be taken into account, so that the partial molar volume v_i of component i in the mixture has to be known. It is obtained here from simple and inexpensive NpT simulations. The proposed procedure yields activity coefficients with low uncertainty and is very robust. It is an advantage of the method that its efficiency does not depend on the studied statepoint, so that it is applicable to systems of low temperature and high density without modifications. Furthermore, it may also be applied to solutions of polymers or proteins, for which algorithms based on particle insertion become very tedious. Using OPAS simulations, the activity of the solvent can be determined with high accuracy. The activity of the solute is then available from the Gibbs-Duhem equation, an approach applied successfully in our previous work on electrolyte solutions.

SUPPLEMENTARY MATERIAL

The supplementary material contains a comparison of the partial molar volumes from molecular simulation and experiment as well as a consistency check of the activity coefficients determined from independent OPAS simulation runs.

ACKNOWLEDGMENTS

The authors gratefully acknowledge financial support within the Reinhart Koselleck Program (HA1993/15-1) of the German Research Foundation (DFG). The present work was

conducted under the auspices of the Boltzmann-Zuse Society of Computational Molecular Engineering (BZS) and the simulations were carried out on the Regional University Computing Center Kaiserslautern (RHRK) under the grant TUKL-TLMV, the High Performance Computing Center Stuttgart (HLRS) under the grant MMHBF as well as the Leibniz Supercomputing Centre (LRZ) under the grant SPARLAMPE (pr48te). The authors thank Stephan Deublein and Steffen Reiser for fruitful discussions.

Appendix A: Simulation Details

All simulations of the present work were carried out with an extended version of the molecular simulation program $ms2$[46]. All simulations employed the velocity scaling thermostat, and electrostatic long-range interactions were calculated using the reaction field method[47,48] with tinfoil boundary conditions. In all simulations, the electrostatic cutoff radius was equal to the Lennard-Jones cutoff radius of 15 Å. In all molecular dynamics (MD) simulations, the time step was 1.2 fs, and the pressure was kept constant in MD NpT simulations using Andersen's barostat. Statistical simulation uncertainties were estimated with the block average method by Flyvbjerg and Petersen[49].

1. OPAS Simulations

OPAS MD simulations were carried out as in previous work[4,5], using 4000 particles. At first, simulations in a modified NpT ensemble were carried out, in which equilibration and production took 2,000,000 and 5,000,000 time steps, respectively. The resulting box volume V was then used for a run in the NVT ensemble, in which equilibration and production took 2,000,000 and 10,000,000 time steps, respectively.

2. Simulations for Molar Excess Volumes

Conventional MD simulations were carried out in the NpT ensemble with 1000 particles. Equilibration and production took 100,000 and 2,000,000 time steps, respectively.

3. Simulations using Thermodynamic Integration

The chemical potential of both components was sampled with thermodynamic integration in Monte Carlo (MC) simulations in the NpT ensemble with 1000 particles, employing an adaptive sampling technique with non-linear scaling as proposed by Kristóf and Rutkai[45] (using 100 bins from $0.2 \leq \lambda \leq 1$, with a maximum λ displacement per attempt of 0.1 and the exponent $d = 4$). These simulations yield the reduced residual chemical potential

$$\tilde{\mu}_i = [\mu_i - \mu_i^{\mathrm{id}}(T)]/(RT), \tag{A1}$$

where $\mu_i^{\mathrm{id}}(T)$ is the part of the ideal chemical potential of component i that only depends on temperature. Activity coefficients are obtained from

$$\ln \gamma_i = \tilde{\mu}_i - \tilde{\mu}_i^{\mathrm{pure}} - \ln x_i. \tag{A2}$$

The fluid was equilibrated for 50,000 MC loops, before sampling was carried out for 9,600,000 MC loops. Each MC loop consisted of $N_{\mathrm{NDF}}/3$ steps, where N_{NDF} indicates the total number of mechanical degrees of freedom of the system, plus one attempt to resize the box according to the Metropolis acceptance criterion.

REFERENCES

[1]B Widom. Some Topics in the Theory of Fluids. *J. Chem. Phys.*, 39:2808–2812, 1963.

[2]M. P. Allen and D. J. Tildesley. *Computer Simulation of Liquids*. Clarendon Press, Oxford, 1991.

[3]D. Frenkel and B. Smit. *Understanding Molecular Simulation: From Algorithms to Applications, 2nd ed.* Academic Press, Elsevier, San Diego, 2002.

[4]M. Kohns, S. Reiser, M. Horsch, and H. Hasse. Solvent activity in electrolyte solutions from molecular simulation of the osmotic pressure. *J. Chem. Phys.*, 144:084112, 2016.

[5]M. Kohns, M. Schappals, M. Horsch, and H. Hasse. Activities in Aqueous Solutions of the Alkali Halide Salts from Molecular Simulation. *J. Chem. Eng. Data*, 61:4068–4076, 2016.

[6]J. Powles, S. Murad, and P. Ravi. A New Model for Permeable Micropores. *Chem. Phys. Lett.*, 188:21–24, 1992.

[7]S. Murad and J. Powles. A Computer Simulation of the Classic Experiment on Osmosis and Osmotic Pressure. *J. Chem. Phys.*, 99:7271–7272, 1993.

[8]S. Murad, J. Powles, and B. Holtz. Osmosis and reverse osmosis in solutions: Monte Carlo simulations and van der Waals one-fluid theory. *Mol. Phys.*, 86:1473–1483, 1995.

[9]F. Paritosh and S. Murad. Molecular simulations of osmosis and reverse osmosis in aqueous electrolyte solutions. *AIChE J.*, 42:2984–2986, 1996.

[10]P. S. Crozier and R. L. Rowley. Activity coefficient prediction by osmotic molecular dynamics. *Fluid Phase Equilib.*, 193:53–73, 2002.

[11]*Dortmund Data Bank, Version 2016*. DDBST GmbH, Oldenburg, 2016.

[12]S. K. Allison, J. P. Fox, R. Hargreaves, and S. P. Bates. Clustering and microimmiscibility in alcohol-water mixtures: Evidence from molecular-dynamics simulations. *Phys. Rev. B*, 71:024201, 2005.

[13]I. Bako, T. Megyes, S. Balint, T. Grosz, and V. Chihaia. Water-methanol mixtures: topology of hydrogen bonded network. *Phys. Chem. Chem. Phys.*, 10:5004–5011, 2008.

[14]A. A. Chialvo and P. T. Cummings. Structure of Mixed-Solvent Electrolyte Solutions via Gibbs Ensemble Monte Carlo Simulation. *Mol. Sim.*, 11:163–175, 1993.

[15]L. Dougan, R. Hargreaves, S. P. Bates, J. L. Finney, V. Reat, A. K. Soper, and J. Crain. Segregation in aqueous methanol enhanced by cooling and compression. *J. Chem. Phys.*, 122:174514, 2005.

[16]M. Ferrario, M. Haughney, I. R. McDonald, and M. L. Klein. Molecular Dynamics Simulation of Aqueous Mixtures - Methanol, Acetone, and Ammonia. *J. Chem. Phys.*, 93:5156–5166, 1990.

[17]L. C. G. Freitas. Monte Carlo Simulation of the Binary Liquid Mixture Water-Methanol. *J. Mol. Struct. (Theochem)*, 101:151–158, 1993.

[18]E. Galicia-Andrés, H. Dominguez, L. Pusztai, and O. Pizio. Composition dependence of thermodynamic, dynamic and dielectric properties of water-methanol model mixtures. Molecular dynamics simulation results with the OPLS-AA model for methanol. *J. Mol. Liq.*, 212:70–78, 2015.

[19]D. Gonzalez-Salgado and I. Nezbeda. Excess properties of aqueous mixtures of methanol: Simulation versus experiment. *Fluid Phase Equilib.*, 240:161–166, 2006.

[20]D. Gonzalez-Salgado, K. Zemankova, E. G. Noya, and E. Lomba. Temperature of maximum density and excess thermodynamics of aqueous mixtures of methanol. *J. Chem. Phys.*, 144:184505, 2016.

[21]G. Guevara-Carrion, J. Vrabec, and H. Hasse. Prediction of self-diffusion coefficient and shear viscosity of water and its binary mixtures with methanol and ethanol by molecular simulation. *J. Chem. Phys.*, 134:074508, 2011.

[22]G. Guevara-Carrion, Y. Gaponenko, T. Janzen, J. Vrabec, and V. Shevtsova. Diffusion in Multicomponent Liquids: From Microscopic to Macroscopic Scales. *J. Phys. Chem. B.*,

120:12193–12210, 2016.

[23]S Hempel, J Fischer, and G Paschek, D Sadowski. Activity Coefficients of Complex Molecules by Molecular SImulation and Gibbs-Duhem Integration. *Soft Mater.*, 10:26–41, 2012.

[24]W. L. Jorgensen and J. D. Madura. Quantum and Statistical Studies of Liquids 25: Solvation and Conformation of Methanol in Water. *J. Am. Chem. Soc.*, 105:1407–1413, 1983.

[25]A. Laaksonen, P. G. Kusalik, and I. M. Svishchev. Three-dimensional structure in water-methanol mixtures. *J. Phys. Chem. A*, 101:5910–5918, 1997.

[26]M. Lisal, W. R. S. William, and I. Nezbeda. Accurate vapour-liquid equilibrium calculations for complex systems using the reaction Gibbs ensemble Monte Carlo simulation method. *Fluid Phase Equilib.*, 181:127–146, 2001.

[27]F. Moučka and I. Nezbeda. Water-methanol mixtures with non-Lorentz-Berthelot combining rules: A feasibility study. *J. Mol. Liq.*, 159:47–51, 2011.

[28]C. Nieto-Draghi, R. Hargreaves, and S. P. Bates. Structure and dynamics of water in aqueous methanol. *J. Phys.: Condens. Matter*, 17:S3265–S3272, 2005.

[29]S. Y. Noskov, M. G. Kiselev, A. M. Kolker, and B. M. Rode. Structure of methanol-methanol associates in dilute methanol-water mixtures from molecular dynamics simulation. *J. Mol. Liq.*, 91:157–165, 2001.

[30]S. Okazaki, K. Nakanishi, and H. Touhara. Computer Experiments on Aqueous Solutions 1: Monte Carlo Calculation on the Hydration of Methanol in an Infinitely Dilute Aqueous Solution with a New Water-Methanol Pair Potential. *J. Chem. Phys.*, 78:454–469, 1983.

[31]S. Okazaki, H. Touhara, and K. Nakanishi. Computer Experiments on Aqueous Solutions 5: Monte Carlo Calculation on the Hydrophobin Interaction in 5 Mol-Percent Methanol

Solution. *J. Chem. Phys.*, 81:890–894, 1984.

[32]T. Ono, K. Horikawa, M. Ota, Y. Sato, and H. Inomata. Insight into the Local Composition of the Wilson Equation at High Temperatures and Pressures through Molecular Simulations of Methanol-Water Mixtures. *J. Chem. Eng. Data*, 59:1024–1030, 2014.

[33]T. A. Pascal and W. A. Goddard, III. Hydrophobic Segregation, Phase Transitions and the Anomalous Thermodynamics of Water/Methanol Mixtures. *J. Phys. Chem. B*, 116:13905–13912, 2012.

[34]J.-C. Soetens and P. A. Bopp. Water-Methanol Mixtures: Simulations of Mixing Properties over the Entire Range of Mole Fractions. *J. Phys. Chem. B*, 119:8593–8599, 2015.

[35]H. J. Strauch and P. T. Cummings. Gibbs Ensemble Simulation of Mixed-Solvent Electrolyte Solutions. *Fluid Phase Equilib.*, 86:147–172, 1993.

[36]H. Tanaka and K. E. Gubbins. Structure and Thermodynamic Properties of Water-Methanol Mixtures - Role of the Water-Water Interaction. *J. Chem. Phys.*, 97:2626–2634, 1992.

[37]H. Tanaka, J. Walsh, and K. E. Gubbins. Structure of Water-Methanol Binary Mixtures - Role of the Water-Water Interaction. *Mol. Phys.*, 76:1221–1233, 1992.

[38]L. Vlcek and I. Nezbeda. Excess properties of aqueous mixtures of methanol: Simple models versus experiment. *J. Mol. Liq.*, 131:158–162, 2007.

[39]E. J. W. Wensink, A. C. Hoffmann, P. J. van Maaren, and D. van der Spoel. Dynamic properties of water/alcohol mixtures studied by computer simulation. *J. Chem. Phys.*, 119:7308–7317, 2003.

[40]H. Yu, D. P. Geerke, H. Liu, and W. E. van Gunsteren. Molecular dynamics simulations of liquid methanol and methanol-water mixtures with polarizable models. *J. Comput. Chem.*, 27:1494–1504, 2006.

[41]Y. Zhong, G. L. Warren, and S. Patel. Thermodynamic and structural properties of methanol-water solutions using nonadditive interaction models. *J. Comput. Chem.*, 29:1142–1152, 2008.

[42]J. L. F. Abascal and C. Vega. A general purpose model for the condensed phases of water: TIP4P/2005. *J. Chem. Phys.*, 123:234505, 2005.

[43]T. Schnabel, A. Srivastava, J. Vrabec, and H. Hasse. Hydrogen bonding of methanol in supercritical CO2: Comparison between H-1 NMR spectroscopic data and molecular simulation results. *J. Phys. Chem. B*, 111:9871–9878, 2007.

[44]W. R. Smith, F. Moucka, and I. Nezbeda. Osmotic pressure of aqueous electrolyte solutions via molecular simulations of chemical potentials: Application to NaCl. *Fluid Phase Equilib.*, 407:76–83, 2016.

[45]T. Kristóf and G. Rutkai. Chemical potential calculations by thermodynamic integration with separation shifting in adaptive sampling Monte Carlo simulations. *Chem. Phys. Lett.*, 445:74–78, 2007.

[46]C. W. Glass, S. Reiser, G. Rutkai, S. Deublein, A. Köster, G. Guevara-Carrión, A. Wafai, M. Horsch, M. Bernreuther, T. Windmann, H. Hasse, and J. Vrabec. ms2: A Molecular Simulation Tool for Thermodynamic Properties, New Version Release. *Comput. Phys. Commun.*, 185:3302–3306, 2014.

[47]J. A. Barker and R. O. Watts. Monte Carlo Studies of Dielectric Properties of Water-like Models. *Mol. Phys.*, 26:789–792, 1973.

[48]B. Saager, J. Fischer, and M. Neumann. Reaction Field Simulations of Monatomic and Diatomic Dipolar Fluids. *Mol. Sim.*, 6:27–49, 1991.

[49]H. Flyvbjerg and H.G. Petersen. Error-estimates on Averages of Correlated Data. *J. Chem. Phys.*, 91:461–466, 1989.

[50]C. Coquelet, A. Valtz, and D. Richon. Volumetric properties of water plus monoethanolamine plus methanol mixtures at atmospheric pressure from 283.15 to 353.15 K. *J. Chem. Eng. Data*, 50:412–418, 2005.

[51]W. Wagner and A. Pruss. The IAPWS formulation 1995 for the thermodynamic properties of ordinary water substance for general and scientific use. *J. Phys. Chem. Ref. Data*, 31:387–535, 2002.

[52]K. de Reuck and R. Craven. *Methanol, International Thermodynamic Tables of the Fluid State - 12.* IUPAC, Blackwell Scientific Publications, London, 1993.

[53]Z. S. Kooner, R. C. Phutela, and D. V. Fenby. Determination of the Equilibrium Constants of Water-Methanol Deuterium Exchange Reactions From Vapor Pressure Measurements. *Aust. J. Chem.*, 33:9–13, 1980.

[54]S. Bernatova, K. Aim, and I. Wichterle. Isothermal vapour-liquid equilibrium with chemical reaction in the quaternary water plus methanol plus acetic acid plus methyl acetate system, and in five binary sub-systems. *Fluid Phase Equilib.*, 247:96–101, 2006.

FIGURES

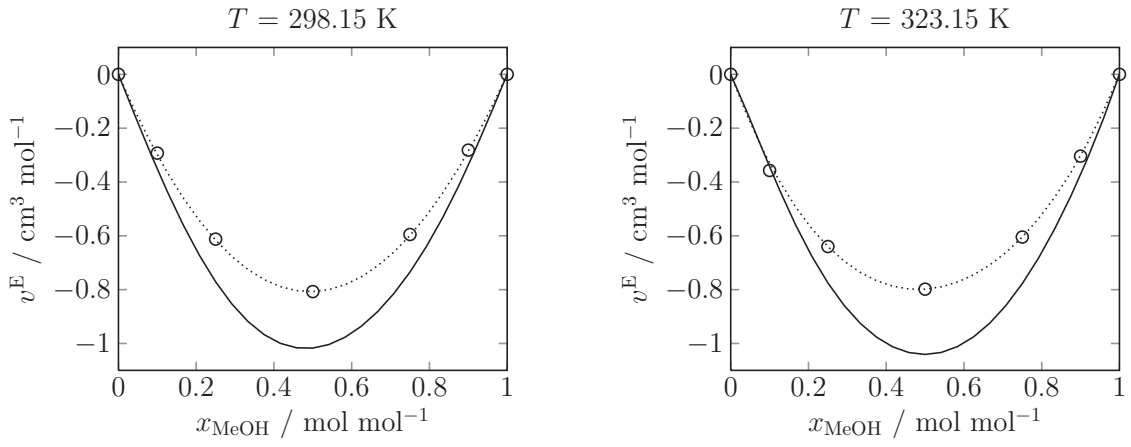

FIG. 1. Molar excess volume of water-methanol mixtures at $p = 1$ bar. Open circles show results from predictive molecular simulations, dotted lines show a Redlich-Kister correlation to these results. Statistical uncertainties are within symbol size. The solid lines are correlations to experimental data by Coquelet et al.[50].

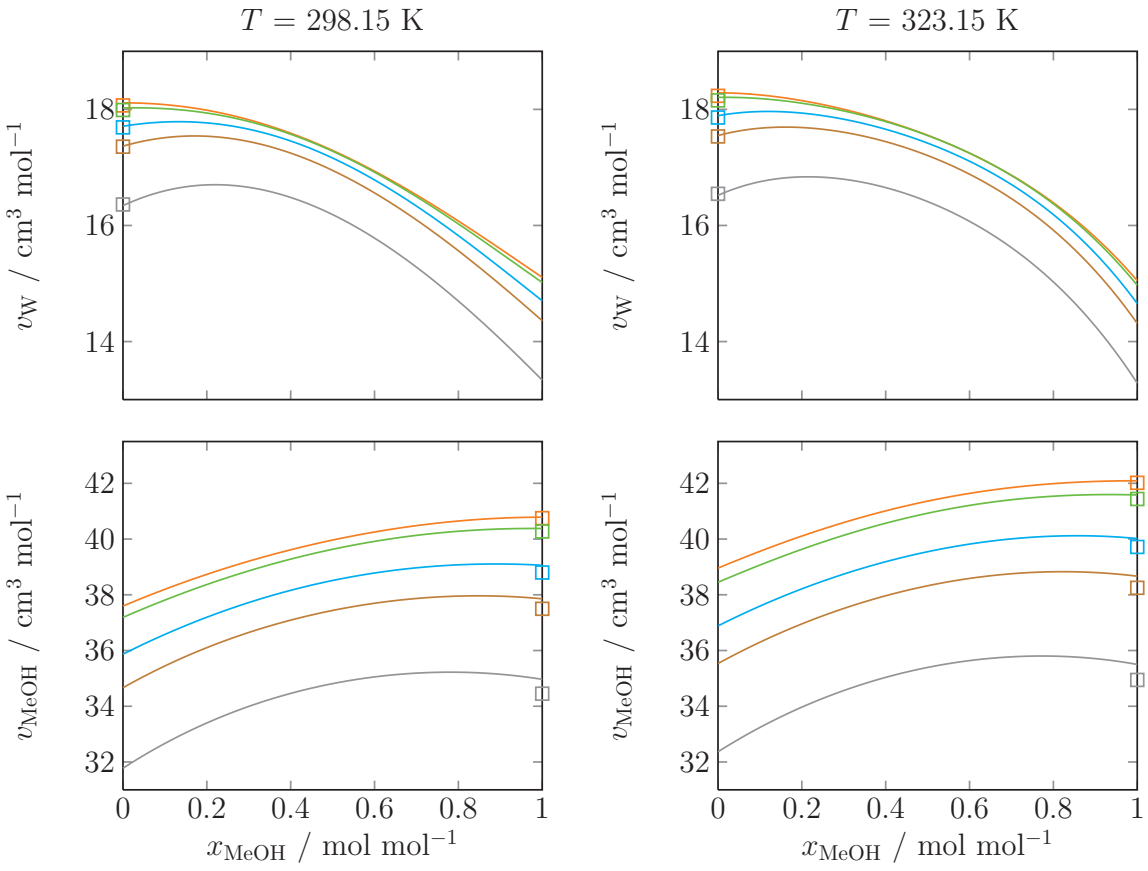

FIG. 2. Partial molar volumes of water (top) and methanol (bottom) in water-methanol mixtures obtained from Redlich-Kister correlations fit to molecular simulation results for the molar excess volumes. Colored lines correspond to different pressures (from top to bottom): (-) $p = 0.1$ MPa, (-) $p = 10$ MPa, (-) $p = 50$ MPa, (-) $p = 100$ MPa, (-) $p = 300$ MPa. The open squares colored accordingly are molar volumes of pure water and pure methanol computed from the equations of state by Wagner and Pruss[51] and by de Reuck and Craven[52], respectively.

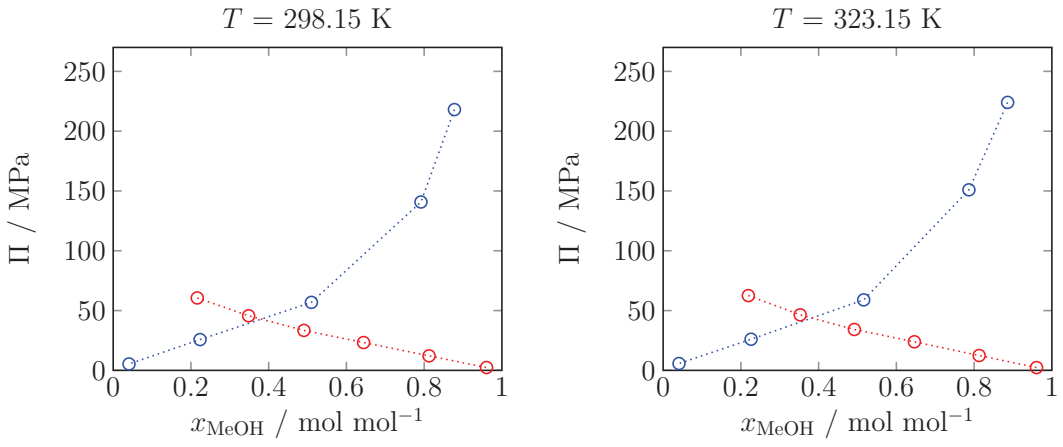

411

412 FIG. 3. Osmotic pressures obtained in OPAS simulations using water as the permeable component
413 (blue) or methanol as the permeable component (red), dotted lines are guides to the eye. Statistical
414 uncertainties are within symbol size.

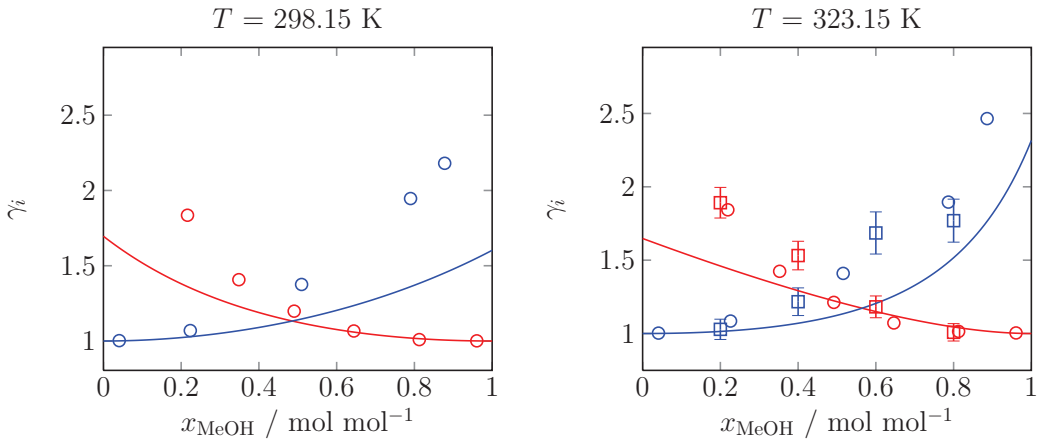

FIG. 4. Activity coefficients of methanol (red) and water (blue) in water-methanol mixtures at $p = 1$ bar. The open circles show simulation results obtained with the OPAS method. Statistical uncertainties of the OPAS simulation results are within symbol size. In the right panel, the open squares show simulation results using the same molecular models, but obtained from sampling the chemical potential with thermodynamic integration. Solid lines show NRTL fits to the experimental data of Kooner et al.[53] (left panel) and by Bernatova et al.[54] (right panel).

TABLES

TABLE I. Densities and parameters of Redlich-Kister correlations, cf. Eq. (12), fit to molar excess volumes for binary mixtures of water and methanol.

	$\rho(T = 298.15\ \mathrm{K})$ / mol l^{-1}					$T = 298.15$ K		
	x_{MeOH} / mol mol^{-1}					Parameters for v^{E} / cm^3 mol^{-1}		
p / MPa	0	0.25	0.5	0.75	1	A_0	A_1	A_2
0.1	55.21(1)	43.16(1)	34.92(1)	28.968(6)	24.519(4)	−3.2292	−0.0916	0.0372
10	55.48(1)	43.384(9)	35.126(8)	29.203(6)	24.766(5)	−2.9315	−0.0829	−0.1153
50	56.47(1)	44.149(9)	35.907(6)	30.021(5)	25.602(4)	−2.1386	0.0819	−0.0695
100	57.59(1)	45.012(8)	36.757(6)	30.850(5)	26.417(3)	−1.6183	0.2426	0.1887
300	61.194(8)	47.756(6)	39.197(5)	33.136(4)	28.600(2)	−0.5657	0.3927	0.2493
	$\rho(T = 323.15\ \mathrm{K})$ / mol l^{-1}					$T = 323.15$ K		
	x_{MeOH} / mol mol^{-1}					Parameters for v^{E} / cm^3 mol^{-1}		
p / MPa	0	0.25	0.5	0.75	1	A_0	A_1	A_2
0.1	54.69(1)	42.259(9)	33.973(7)	28.123(6)	23.758(5)	−3.0137	0.0507	−0.2649
10	54.93(1)	42.517(8)	34.228(8)	28.390(5)	24.048(4)	−2.7153	−0.0796	−0.2904
50	55.896(9)	43.378(7)	35.138(6)	29.310(4)	24.989(3)	−1.9799	−0.0070	0.0629
100	56.99(1)	44.314(6)	36.047(5)	30.205(4)	25.862(3)	−1.4650	0.1003	0.0757
300	60.538(6)	47.157(5)	38.641(4)	32.639(3)	28.169(2)	−0.5199	0.3133	0.2183

TABLE II. Results of OPAS simulations and deduced activity coefficients. The upper block shows results of simulations with methanol as the permeable component, the lower block shows results of simulations with water as the permeable component.

$T = 298.15$ K			$T = 323.15$ K		
x_{MeOH} / mol mol^{-1}	Π / MPa	γ_{MeOH}	x_{MeOH} / mol mol^{-1}	Π / MPa	γ_{MeOH}
0.2163(5)	60.6(3)	1.84(1)	0.2192(6)	62.5(3)	1.84(1)
0.3484(5)	45.7(3)	1.407(6)	0.3525(5)	46.4(2)	1.42(6)
0.4907(5)	33.4(2)	1.198(4)	0.4919(4)	34.2(2)	1.212(4)
0.6442(2)	23.3(2)	1.067(3)	0.6463(2)	23.9(1)	1.072(2)
0.8126(1)	12.1(1)	1.009(2)	0.8129(1)	12.4(1)	1.014(2)
0.9605(1)	2.382(5)	1.0011(8)	0.9606(1)	2.33(5)	1.0039(8)
x_{MeOH} / mol mol^{-1}	Π / MPa	γ_{W}	x_{MeOH} / mol mol^{-1}	Π / MPa	γ_{W}
0.8779(8)	218.0(5)	2.18(1)	0.8862(8)	224.1(5)	2.46(1)
0.7901(8)	140.9(4)	1.946(7)	0.7866(8)	151.0(5)	1.896(7)
0.5098(7)	56.9(4)	1.376(4)	0.5159(7)	58.9(3)	1.410(3)
0.2235(4)	25.8(2)	1.069(2)	0.2262(4)	26.0(2)	1.085(2)
0.0407(1)	5.36(9)	1.0025(7)	0.0408(1)	5.72(9)	1.0028(7)

429 TABLE III. Reduced residual chemical potentials and activity coefficients of water and methanol

430 at $T = 323.15$ K and $p = 1$ bar obtained from thermodynamic integration.

x_{MeOH} / mol mol^{-1}	$\tilde{\mu}_{\mathrm{MeOH}}$	$\tilde{\mu}_{\mathrm{W}}$	γ_{MeOH}	γ_{W}
0	–	−10.40(6)	–	1
0.2	−8.68(6)	−10.60(7)	1.9(1)	1.03(7)
0.4	−8.20(6)	−10.72(8)	1.5(1)	1.22(9)
0.6	−8.05(6)	−10.79(9)	1.18(7)	1.7(1)
0.8	−7.92(6)	−11.44(8)	1.01(6)	1.8(1)
1	−7.71(6)	–	1	–

Supplementary Material to:

Activity Coefficients from Molecular Simulations using the OPAS Method

Maximilian Kohns, Martin Horsch, and Hans Hasse

1 Comparison of Partial Molar Volume Results to Experimental Data

In the literature, two sets of experimental data on densities or molar excess volumes of mixtures of water and methanol at elevated pressures exist: Safarov et al. [1] studied the system at pressures up to $p = 60$ MPa and report data for $T = 298.15$ K and $T = 323.15$ K. Yokoyama et al. [2] studied the system at pressures up to $p = 200$ MPa, but report data only at $T = 320$ K and higher temperatures. However, $T = 320$ K seems close enough to $T = 323.15$ K to enable at least a qualitative comparison with our molecular simulation predictions.

Both groups only give numbers for the densities or molar volumes, respectively. Thus, they were correlated with a Redlich-Kister approach, similar to the treatment of the molecular simulation data discussed in the main text, and the partial molar volumes were computed from these correlations. To enable this, the data of Safarov et al. [1] were complemented with the pure component molar volumes computed from the equations of state by Wagner and Pruss [3] for water and de Reuck and Craven [4] for methanol, respectively. Yokoyama et al. [2] report data for pure methanol, which were used here, and their data set was also complemented

with the equation of state of Wagner and Pruss [3] for water. The partial molar volumes obtained in this manner are shown in Figs. S1 and S2, respectively, where they are compared to the predictions from molecular simulations already discussed in the main text.

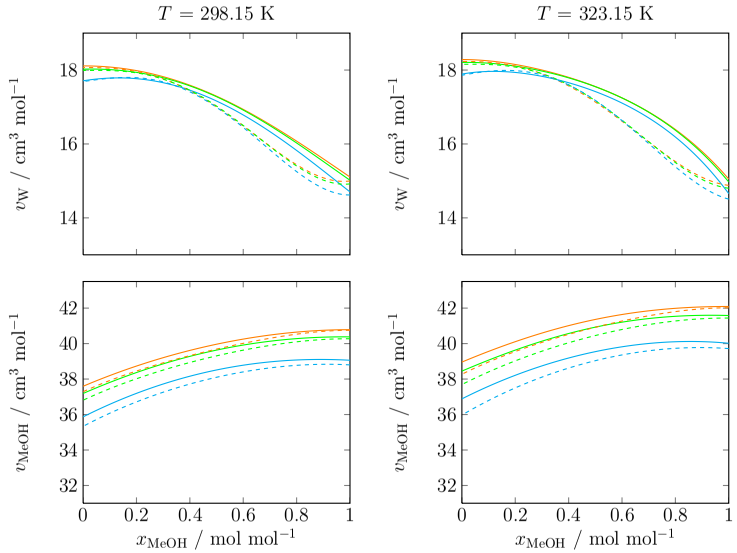

Figure S1: Partial molar volumes of water (top) and methanol (bottom) in water-methanol mixtures obtained from Redlich-Kister correlations. Solid lines: fit to molecular simulation results for the molar excess volumes. Dashed lines: Fit to experimental data by Safarov et al. [1]. Colors correspond to different pressures (from top to bottom): (-) $p = 0.1$ MPa, (-) $p = 10$ MPa, (-) $p = 50$ MPa.

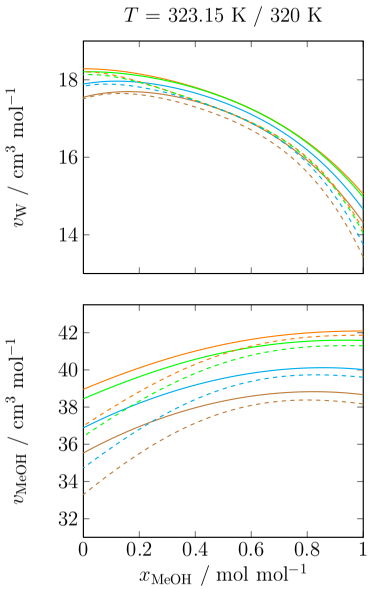

Figure S2: Partial molar volumes of water (top) and methanol (bottom) in water-methanol mixtures obtained from Redlich-Kister correlations. Solid lines: fit to molecular simulation results for the molar excess volumes, $T = 323.15$ K. Dashed lines: Fit to experimental data by Yokoyama et al. [2], $T = 320$ K. Colors correspond to different pressures (from top to bottom): (-) $p = 0.1$ MPa, (-) $p = 10$ MPa, (-) $p = 50$ MPa, (-) $p = 100$ MPa.

The molecular simulation predictions of v_{MeOH} (bottom panels in both figures) compare favorably with both sets of experimental data. The qualitative dependence of v_{MeOH} on x_{MeOH} is predicted correctly. This is true for all isobars. However, the molecular simulation predictions show a quantitative offset from the experimental data, which mainly arises from the differences in $v_{\mathrm{MeOH}}^{\mathrm{pure}}$ already discussed in the main text. Additionally, the partial molar volume of methanol at infinite dilution in water $v_{\mathrm{MeOH}}^{\infty}$ seems to be slightly underpredicted.

Regarding v_{W} (top panels in both figures), the agreement between the molecular simulation predictions and the experimental data is very good in the water-rich region. In the methanol-rich region, however, the two sets of experimental data disagree. It is therefore difficult to assess the molecular simulation predictions. If compared to the experimental data of Safarov et al. [1] (Fig. S1), the numbers for the partial molar volume of water at infinite dilution in methanol v_{W}^{∞} are predicted correctly, but the dependence of v_{W} on x_{MeOH} is not depicted correctly. If compared to the experimental data of Yokoyama et al. [2] (Fig. S2), the prediction of the trend is very good, whereas the numbers found for $v_{\mathrm{MeOH}}^{\infty}$ are too low.

Altogether, taking into account that the employed molecular models are conceptually simple and no adjustment to experimental data of the binary system was made, the predictions of the partial molar volumes are quite satisfactory.

2 NRTL Fit to Simulation Results

In order to check the thermodynamic consistency of the values for γ_{W} and γ_{MeOH} obtained from independent OPAS simulation runs, an NRTL model was fit to the data, cf. Fig. S3. For both temperatures, the data and the fits agree well, which shows the consistency of the OPAS simulation results.

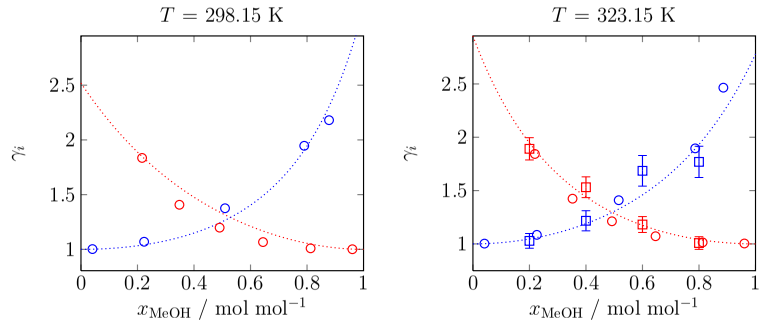

Figure S3: Activity coefficients of methanol (red) and water (blue) in water-methanol mixtures at $p = 1$ bar. The open circles show simulation results obtained with the OPAS method. Statistical uncertainties of the OPAS simulation results are within symbol size. In the right panel, the open squares show simulation results using the same molecular models, but obtained from sampling the chemical potential with thermodynamic integration. Dotted lines show a simultaneous fit to the OPAS simulation results for the activity coefficients of both components using an NRTL model.

References

[1] J. Safarov, S. Heydarov, A. Shahverdiyev, and E. Hassel. Excess molar volumes V_m^E, isothermal compressibilities k, and thermal expansivities α of $\{(1\text{-}x)H_2O+xCH_3OH\}$ at T =(298.15 to 523.15) K and pressures up to 60 MPa. *J. Chem. Thermodynamics*, 36:541–547, 2004.

[2] H. Yokoyama and M. Uematsu. Thermodynamic properties of $\{xCH_3OH+(1\text{-}x)H_2O\}$ at x = (1.0000, 0.8005, 0.4002, and 0.2034) in the temperature range from 320 K to 420 K at pressures up to 200 MPa. *J. Chem. Thermodynamics*, 35:813–823, 2003.

[3] W. Wagner and A. Pruss. The IAPWS formulation 1995 for the thermodynamic properties of ordinary water substance for general and scientific use. *J. Phys. Chem. Ref. Data*, 31:387–535, 2002.

[4] K. de Reuck and R. Craven. *Methanol, International Thermodynamic Tables of the Fluid State - 12*. IUPAC, Blackwell Scientific Publications, London, 1993.